Axial Buckling of Pressurized Imperfect Cylindrical Shells*

by

John Hutchinson

Harvard University, Cambridge, Mass.

Abstract

While some experiments seem to confirm the contention that the axial buckling load of a pressurized cylinder approaches the classical value (i.e., the value predicted by the linear buckling equations) for sufficiently large internal pressure, other tests indicate a much smaller buckling load increase resulting from pressurization. Here it is shown that the buckling load of an elastic shell with asymmetric imperfections but sufficiently free of axisymmetric imperfections closely coincides with the classical value for relatively small values of internal pressure; while the buckling load of a shell with a predominance of axisymmetric imperfection can remain well below the classical value for the entire range of internal pressures for which the shell buckles elastically. Of particular interest is the calculation of an upper bound to the buckling load as predicted by the non-linear Donnell-shell equations for a shell with axisymmetric imperfections.

* This work was supported by the National Aeronautics and Space Administration under Contract No. NsG-559 with Harvard University.

INTRODUCTION

The several published analyses of pressurized cylindrical shells under axial compression do not adequately explain the variety of behavior which has been reported for such structures. The linear buckling equations predict that the buckling parameter

$$\lambda = \sqrt{3(1 - \nu^2)}\ \frac{R}{Eh}\ (\sigma - \frac{pR}{2h})$$

is unity for pressurized and unpressurized shells. Here σ is the applied compressive stress and $pR/2h$ is the axial stress resulting from pressurization as depicted in Figure 1. Experiments indicate that this buckling parameter is usually on the order of one half or one third for unpressurized shells and is larger for pressurized shells. In some tests the parameter is unity for shells under sufficient internal pressure, while in other cases this parameter remains well below unity for the entire range of pressures for which the shell buckles elastically.

Lo, Crate and Schwartz (1) used non-linear buckling equations for a perfect shell and employed the energy criteria of buckling to show that the buckling parameter, as defined here, increases from .62 at $p = 0$ to unity at $pR^2/Eh^2 = .17$. Thieleman (2) also reported calculations for initially perfect shells based on a non-linear analysis. He obtains load-deflection curves from which is obtained the minimum load the shell can support following buckling. This minimum load increases with increased internal pressure.

The role of shell imperfections, known to be the main degrading factor in unpressurized shells, was not considered in either of the above mentioned papers. Lu and Nash (3) have studied the effect of initial imperfections on the minimum

load the shell can support in the post-buckling region. This analysis also shows a larger minimum load for pressurized shells than unpressurized ones.

From a design stand-point, the maximum load the shell can support prior to buckling is of more interest than the minimum post-buckling load. Indeed, it is this value which most experimenters record and which we will designated as the buckling load in this report. Here, approximate solutions to the non-linear, Donnell-type shell equations will be obtained which display the role of axisymmetric and asymmetric imperfections on the buckling load of a pressurized elastic shell. It will be seen that axisymmetric imperfections of a certain wavelength are particularly degrading. An upperbound to the exact buckling load as predicted by the non-linear equations is obtained for the case of axisymmetric imperfections. Finally, these solutions are compared with some experimental results, and it is noted that they seem to account for the variety of reported behavior.

DONNELL SHELL EQUATIONS

The elastic shell is characterized by its radial displacement W (positive outward) and an Airy stress function F which gives the resultant membrane stresses as $N_{xx} = F_{,yy}$, $N_{yy} = F_{,xx}$ and $N_{xy} = -F_{,xy}$. The shell is assumed to have an initial imperfection in the form of an initial, stress-free radial displacement W_o. With x and y as the cartesian coordinates in the axial and circumferential directions, the equations are

$$\frac{1}{Eh}\nabla^4 F - \frac{1}{R}W_{,xx} + (W_{o,xx} + W_{,xx})W_{,yy} + W_{o,yy}W_{,xx} - W^2_{,xy} - 2W_{o,xy}W_{,xy} = 0 \qquad (1)$$

and

$$\frac{Eh^3}{12(1-\nu^2)}\nabla^4 W + \frac{1}{R}F_{,xx} - (W_{o,xx} + W_{,xx})F_{,yy} - (W_{,yy} + W_{o,yy})F_{,xx} + 2W_{o,xy}F_{,xy}$$

$$+ 2W_{,xy}F_{,xy} - p = 0 \qquad (2)$$

where ∇^4 is the two dimensional biharmonic operator.

CLASSICAL BUCKLING

We consider a perfect cylinder ($W_o = 0$) under internal pressure p and axial compressive stress σ (in addition to the axial stress resulting from the internal pressure). The state of deformation can be written as

$$W = \frac{\nu}{E}(\sigma h + \frac{pR}{2}) + \frac{1}{E}pR + w \qquad (3)$$

$$F = (-\frac{1}{2}\sigma h + \frac{1}{4}pR)y^2 + \frac{1}{2}pRx^2 + f \qquad (4)$$

where the terms added to w and f constitute the prebuckling solution for the perfect shell. The classical buckling equations are obtained by substituting (3) and (4) in the Donnell-shell equations and then linearizing the resulting equations with respect to w and f. The linear buckling equations are

$$\frac{1}{Eh}\nabla^4 f - \frac{1}{R}w_{,xx} = 0 \qquad (5)$$

$$\frac{Eh^3}{12(1-\nu^2)}\nabla^4 w + (h\sigma - \frac{pR}{2})w_{,xx} - pRw_{,yy} + \frac{1}{R}f_{,xx} = 0 \qquad (6)$$

Solutions to these equations are well known.* The eigen-value

$$\lambda = \frac{\sigma q_o^2}{2E} - \frac{\bar{p}}{2} = \frac{1}{2}\left(\frac{(\alpha^2 + \beta^2)^2}{\alpha^2} + \frac{\alpha^2}{(\alpha^2 + \beta^2)^2}\right) + \bar{p}\left(\frac{\beta}{\alpha}\right)^2 \qquad (7)$$

corresponds to a radial deflection mode of the form

$$w = \cos(\alpha q_o x/R)\cos(\beta q_o y/R) \qquad (8)$$

and the associated stress function

$$f = -\frac{ERh}{q_o^2}\,\frac{\alpha^2}{(\alpha^2 + \beta^2)^2}\,\cos(\alpha q_o x/R)\cos(\beta q_o y/R) \qquad (9)$$

where

$$q_o^4 = 12(1 - \nu^2)R^2/h^2 \qquad \text{and} \qquad \bar{p} = \frac{pR^2}{Eh^2}\sqrt{3(1 - \nu^2)}\ .$$

The classical buckling parameter for the <u>unpressurized</u> shell, obtained by minimizing λ as given by equation (7) with respect to α and β, is

$$\lambda_c^o = \frac{\sigma q_o^2}{2E} = 1 \qquad (10)$$

*In this paper we will assume the shell is sufficiently long to justify neglecting the boundary conditions at the ends of the shell. For certain end conditions Hoff (4) has produced a solution to the linear buckling equations which predicts buckling at $\lambda = 1/2$ for an unpressurized cylindrical shell. It is not known if the post-buckling behavior in this case is unstable, nor is it clear that the shell is significantly imperfection-sensitive for buckling in this mode. Although in certain instances the shell buckling may be characterized by the solution obtained by Hoff, we will assume that shell imperfections result in the main reduction of the buckling load below what is generally accepted as the "classical" value, $\lambda = 1$.

with an infinite number of associated buckling modes such that α and β satisfy

$$\alpha^2 + \beta^2 - \alpha = 0 \qquad (11)$$

Included in this set of critical buckling modes are the axisymmetric mode $w = \cos(q_o x/R)$ and the asymmetric mode $w = \cos(\frac{1}{2} q_o x/R)\cos(\frac{1}{2} q_o y/R)$.

The classical buckling load (i.e., value of buckling parameter) for the pressurized shell is also unity

$$\lambda_c = \frac{\sigma q_o^2}{2E} - \frac{\bar{p}}{2} = 1$$

however only the axisymmetric mode, $w = \cos(q_o x/R)$, is associated with this critical value. All other modes of the form of equation (8) are associated with eigenvalues larger than unity. Thus, for example, corresponding to $w = \cos(\frac{1}{2} q_o x/R)\cos(\frac{1}{2} q_o y/R)$ is the eigen-value $\lambda = 1 + \bar{p}$.

NON-LINEAR BUCKLING EQUATIONS

We must turn to the non-linear equations and the effect of initial imperfections to explain the discrepancy between the predictions of the linear or classical theory and common experimental observations. It is of particular interest that Koiter (5) has presented an analytic procedure for obtaining the role of imperfections in imperfection-sensitive structures. This work is perhaps more readily available in reference (6) or in a less general form in reference (7). His general theory for cylindrical shells (8) indicates that an imperfection in the form of the radial displacement component of the axisymmetric buckling mode, $W = \mu\cos(q_o x/R)$, is the most degrading and is able to reduce the buckling load of an unpressurized shell under axial compression to one half or even one third the classical value for values of μ only a fraction of the shell thickness.

In general any radial imperfection pattern of the shell can be represented by a double Fourier series in the axial and circumferential coordinates. We will restrict ourselves to a consideration of just two terms of such a series - one axisymmetric and one asymmetric. Both are taken to be in the form of a radial displacement component of a linear buckling mode of the unpressurized shell.

Thus, we study the behavior of a pressurized cylindrical shell under an applied axial load where the initial imperfection is assumed to be

$$W_o = - \bar{\xi}_1 h \cos(q_o x/R) + \bar{\xi}_2 h \cos(\tfrac{1}{2} q_o x/R)\cos(\tfrac{1}{2} q_o y/R) \qquad (12)$$

where $\bar{\xi}_1$ and $\bar{\xi}_2$ are the ratios of the amplitude of the imperfection to the shell thickness.

Any equilibrium state of the axially loaded cylinder can be written in the form of (3) and (4); we approximate w by

$$w = \xi_1 h \cos(q_o x/R) + \xi_2 h \cos(\tfrac{1}{2} q_o x/R)\cos(\tfrac{1}{2} q_o y/R) + \xi_3 h \sin(\tfrac{1}{2} q_o x/R)\cos(\tfrac{1}{2} q_o y/R) \qquad (13)$$

Here ξ_1, ξ_2 and ξ_3 are the ratios of the amplitude of the deflection in the axisymmetric or asymmetric modes to the shell thickness.

Solutions to the full non-linear equations (1) and (2) are obtained in the following manner. First, since equation (1) is a compatibility eq. 1, it is solved exactly for F in terms of the assumed W. This is accomplished with the aid of equations (3) and (4). Since we are ignoring the end conditions and as the average stresses in the shell are given by the polynomial terms in (4), f is required to be the sum of terms periodic in the axial and circumferential

directions. Secondly, we solve equation (2) (an equilibrium equation) approximately by substituting in F and W and then applying the Galkerin procedure. The steps of this calculation are easily carried out and the resulting equations are

$$\xi_1(1 - \lambda) + \frac{3}{32} c\left(\xi_2^2 - \xi_3^2\right) + \frac{1}{8} c\xi_2\bar{\xi}_2 + \lambda\bar{\xi}_1 + \frac{13}{200} c^2 (\bar{\xi}_2 + \xi_2)(\bar{\xi}_2\xi_1 + (\xi_1 - \bar{\xi}_1)\xi_2)$$

$$+ \frac{13}{200} c^2(\xi_1 - \bar{\xi}_1)\xi_3^2 = 0 \qquad (14)$$

$$\xi_2(1 + \bar{p} - \lambda) + \frac{3}{2} c\xi_1\xi_2 - c\xi_2\bar{\xi}_1 + c\xi_1\bar{\xi}_2 + (\bar{p} - \lambda)\bar{\xi}_2 + \frac{13}{25} c^2(\xi_1 - \bar{\xi}_1)(\xi_1\bar{\xi}_2 + \xi_2(\xi_1 - \bar{\xi}_1))$$

$$+ \frac{1}{8} c^2(\xi_2 + \bar{\xi}_2)(\xi_2\bar{\xi}_2 + \frac{1}{2}\xi_2^2) = 0 \qquad (15)$$

and

$$\xi_3(1 + \bar{p} - \lambda) - \frac{3}{2} c\xi_1\xi_3 + c\xi_3\bar{\xi}_1 + \frac{13}{25} c^2(\xi_1 - \bar{\xi}_1)^2\xi_3 + \frac{1}{16} c^2\xi_3^3 = 0 \qquad (16)$$

where $c = \sqrt{3(1 - \nu^2)}$.

A solution to these equations would provide the equilibrium configuration of the shell as a function of λ, i.e. ξ_1, ξ_2 and ξ_3 as a function of λ. If λ attains a maximum as the compressive axial load is applied then this is the value of λ associated with the buckling load. It will be denoted by λ_M. The essential character of the shell behavior in the prebuckling and immediate post-buckling description is retained if the terms of order $\bar{\xi}\xi^2$, $\xi\bar{\xi}^2$ and ξ^3 are omitted from the previous three equations. With this simplification the equations to be studied are

$$\xi_1(1 - \lambda) + \frac{3}{32} c(\xi_2^2 - \xi_3^2) + \frac{1}{8} c\bar{\xi}_2\xi_2 = -\lambda\bar{\xi}_1 \qquad (17)$$

$$\xi_2(1 + \bar{p} - \lambda) + \frac{3}{2} c\xi_1\xi_2 - c\xi_2\bar{\xi}_1 + c\xi_1\bar{\xi}_2 = (\lambda - \bar{p})\bar{\xi}_2 \qquad (18)$$

and

$$\xi_3(1 + \bar{p} - \lambda) - \frac{3}{2} c\xi_1\xi_3 + c\xi_3\bar{\xi}_1 = 0 \qquad (19)$$

For sufficiently small $\bar{\xi}_1$ and $\bar{\xi}_2$, these equations yield a buckling load which is asymptotic to that predicted by (14), (15) and (16) if $\bar{p} = 0$. If $\bar{p} > 0$ we cannot make this assertion; however, the upperbound solution for the case of axisymmetric imperfections obtained in a later section indicates that these equations provide a sufficiently accurate estimate of the buckling load for the purposes of this paper.

The behavior of the perfect shell as predicted by these equations is shown in Figure 2. A perfect shell suffers no deformation in the buckling modes ($\xi_1=\xi_2=\xi_3=0$) until λ reaches unity. With λ remaining at unity, deformation can occur in the axisymmetric mode; and since $\bar{\xi}_1 = 0$, ξ_1 can take on either positive or negative values. If as shown in Figure 2 ξ_1 attains the value $-2\bar{p}/3c$ the coefficient of ξ_2 in equation (18) vanishes and a bifurcation of the solution occurs. The bifurcated solution corresponds to falling values of λ with deformation in both the ξ_1 and ξ_2 modes. If the deformation is such that ξ_1 attains the value $2\bar{p}/3c$, then the coefficient of ξ_3 equation (19) vanishes and λ falls with deformation in the ξ_1 and ξ_3 modes. In either case, the maximum value of λ attained is the classical value, $\lambda = 1$.

AXISYMMETRIC IMPERFECTION

If the imperfection is purely axisymmetric ($\bar{\xi}_2 = 0$, $\bar{\xi}_1 > 0$) the prebuckling deformation is also purely axisymmetric. From (17)

$$\xi_1 = -\frac{\lambda}{1 - \lambda}\bar{\xi}_1$$

and $\xi_2=\xi_3=0$ until there is a bifurcation of the solution which occurs when the coefficient of ξ_2 in (18)

$$1 + \bar{p} - \lambda + \frac{3}{2} c\xi_1 - c\bar{\xi}_1$$

vanishes. Following bifurcation the value of λ falls with deformation occuring in the ξ_2 as well as the axisymmetric mode. This behavior is also depicted in Figure 2. The maximum value of λ, denoted by λ_M, occurs at bifurcation and is found from the previous two equations to be

$$2(1 + \bar{p} - \lambda_M)(1 - \lambda_M) - (2 + \lambda_M)c\bar{\xi}_1 = 0 \quad * \qquad (20)$$

The buckling load for an unpressurized shell is given by

$$2(1 - \lambda_M^\circ)^2 - (2 + \lambda_M^\circ)c\bar{\xi}_1 = 0 \quad . \qquad (21)$$

and is shown as the dashed curve in Figure 3 where it can be compared with an upper-bound solution obtained in a later section. λ_M vs $\bar{p}$ curves obtained from (20) are given in Figure 4. For this plot values of $\bar{\xi}_1$ have been chosen such that the unpressurized shells buckle at $\lambda = .3, .5$ and $.7$. These curves as well as all others in this paper are calculated with $\nu = 1/3$.

ASYMMETRIC AND AXISYMMETRIC IMPERFECTIONS

If both $\bar{\xi}_1$ and $\bar{\xi}_2$ are non-zero, deformation occurs in both the ξ_1 and ξ_2 modes for any non-zero values of $\bar{p}$ and λ. Non-zero values of ξ_3 can

*If $\bar{\xi}_1 < 0$, the coefficient of ξ_3 in (19) vanishes when λ reaches λ_M and the bifurcated solution corresponds to falling values of λ with deformation in the ξ_1 and ξ_3 modes. λ_M is thus dependent only on the absolute value of $\bar{\xi}_1$.

occur only if the coefficient of ξ_3 in equation (19) vanishes, which for the moment we will assume does not happen.

An expression relating λ and ξ_2 can be obtained by eliminating ξ_1 from the two equilibrium equations (17) and (18). This is

$$\lambda^2(\xi_2 + \bar{\xi}_2) - \lambda[\xi_2(2 + \bar{p}) + \bar{\xi}_2(1 + \bar{p}) + \bar{\xi}_1(\frac{1}{2} c\xi_2 + c\bar{\xi}_2)]$$

$$+ (1 + \bar{p})\xi_2 - (\frac{3}{2} c\xi_2 + c\bar{\xi}_2)(\frac{3}{32} c\xi_2^2 + \frac{1}{8} c\xi_2\bar{\xi}_2) - c\xi_2\bar{\xi}_1 + \bar{p}\xi_2 = 0 \qquad (22)$$

A maximum value of λ (if it occurs) is associated with $\frac{d\lambda}{d\xi_2} = 0$. This condition along with (22) yields an expression for λ_M analogous to (20) but considerably more complicated. It was found more convenient to obtain λ_M from a plot of λ vs. ξ_2 using (22). If $\bar{\xi}_1$ is positive and large compared to $\bar{\xi}_2$, ξ_1 assumes only negative values and the coefficient of ξ_3 in equation (19)

$$(1 + \bar{p} - \lambda) - \frac{3}{2} c\xi_1 + c\bar{\xi}_1 \qquad (23)$$

does not vanish. However, when $\bar{\xi}_1$ is zero or small compared to $\bar{\xi}_2$ negative values of ξ_1 are possible; and for sufficiently large values of $\bar{p}$ it was found that this coefficient vanished for a value of λ less than the λ_M provided by (22). Furthermore, in these cases it was found that the bifurcated solution resulted in λ decreasing with deformation in the ξ_3 as well as ξ_1 and ξ_2 modes. In such cases the maximum value of λ attained is that for which (23) vanishes.

The indicated calculations were carried out for several combinations of $\bar{\xi}_1$ and $\bar{\xi}_2$; and the maximum value of λ, λ_M, was obtained over a range of $\bar{p}$ from 0 to 4. λ_M vs $\bar{p}$ curves are shown in the three plots of Figure 5.

In the first plot the combinations of $\bar{\xi}_1$ and $\bar{\xi}_2$ are such that the unpressurized cylinders buckle at $\lambda_M = .7$, while the other two plots depict cylinders which buckle at .5 and .3 when free of internal pressure. The curves of Figure 4 are also included.

It is clear that prediction of the buckling load of a pressurized cylinder requires knowledge of the relative amount of axisymmetric imperfection of the wave length $R/2\pi q_o$. In effect, the asymmetric imperfections are ironed out by the pressure while the axisymmetric ones are not. If $\bar{\xi}_1/\bar{\xi}_2$ is small λ_M is almost the classical value when $\bar{p}$ is near unity. If, however, the initial imperfection is purely axisymmetric the buckling load is much less influenced by internal pressure as indicated by the curves $\bar{\xi}_1/\bar{\xi}_2 = \infty$.

AN UPPER BOUND FOR THE CASE OF AXISYMMETRIC IMPERFECTION

The previous approximate analyses bares the role of the axisymmetric imperfection of wave length $R/2\pi q_o$. Not only does it have the largest degrading effect for the unpressurized shell, for buckling with $\bar{p} > 1$ it almost completely determines the buckling load. With relatively little difficulty an upperbound to the buckling load as predicted by the non-linear Donnell-shell equations can be obtained for a cylindrical shell with axisymmetric imperfections. This is of particular interest in light of the role of such imperfections and the approximate nature of the previous calculations.

Only the steps of this calculation will be recorded here since the details of a similar calculation for unpressurized shells have been given by Koiter (8). If the imperfection is of the form

$$W_o = - \bar{\xi}_1 h \cos(q_o x/R) \quad ,$$

the state of deformation of the shell can be written as

$$W = \left\{ \frac{2\nu h\lambda}{q_o^2} + (1 + \nu)\frac{pR}{E} - \frac{\lambda\bar{\xi}_1 h}{1 - \lambda}\cos(q_o x/R) \right\} + w \qquad (24)$$

$$F = \left\{ -\frac{Eh\lambda y^2}{q_o^2} + \frac{1}{2}pRx^2 + \frac{E\lambda\bar{\xi}_1 h^2 R}{q_o^2(1 - \lambda)}\cos(q_o x/R) \right\} + f \qquad (25)$$

where the terms in the brackets are the <u>exact</u> prebuckling solution to the non-linear Donnell-shell equations (1) and (2). Prior to buckling, w and f are zero. Buckling occurs with the first deviation from the axisymmetric prebuckling deformation. Thus, we look for the value of the load parameter λ at which the non-linear shell equations admit non-zero solutions for w and f. Substituting (24) and (25) in (1) and (2) and linearizing with respect to w and f (we are looking for infinitesimal deviations from zero) we find

$$\frac{1}{Eh}\nabla^4 f - \frac{1}{R}w_{,xx} + \frac{\bar{\xi}_1 h q_o^2}{R^2(1 - \lambda)}\cos(q_o x/R)\, w_{,yy} = 0 \qquad (26)$$

$$\frac{Eh^3}{12(1 - \nu^2)}\nabla^4 w + \frac{1}{R}f_{,xx} - \frac{\bar{\xi}_1 q_o^2 h}{R^2(1 - \lambda)}\cos(q_o x/R)\, f_{,yy} + \frac{E\lambda\bar{\xi}_1 h^2}{R(1 - \lambda)}\cos(q_o x/R) w_{,yy}$$

$$+ \frac{2E\lambda h}{q_o^2}w_{,xx} - pRw_{,yy} = 0 \qquad (27)$$

An exact solution to these equations is not found; however, an approximate method is employed which guarantees that the estimate of the buckling stress is an upperbound to the exact buckling stress. Assume

$$w = \xi h \cos(q_o x/2R)\cos(\gamma q_o y/2R) \qquad (28)$$

Solve the compatibility equation (26) exactly for f in terms of the assumed w. f must be the sum of terms periodic in the axial and circumferential direction since we have ignored the end conditions and the average stresses in the shell are represented by the polynomial terms in F in equation (25). Then apply the Galkerin procedure to equation (27). This method of solution is equivalent to an approximate minimization of the second variation of the energy by the Raleigh-Ritz method, which ensures that the eigen-value so obtained is an upperbound to the buckling stress.* This straightforward calculation yields the following eigen-value equation

$$(1 - \lambda)^2\left[\frac{(1 + \gamma^2)^2}{4} + \frac{4}{(1 + \gamma^2)^2} + 2\bar{p}\gamma^2 - 2\lambda\right] - c\gamma^2\bar{\xi}_1(1 - \lambda)\left(\lambda + \frac{8}{(1 + \gamma^2)^2}\right)$$

$$+ 4(c\gamma^2\bar{\xi}_1)^2\left[\frac{1}{(1 + \gamma^2)^2} + \frac{1}{(9 + \gamma^2)^2}\right] = 0 \tag{29}$$

The approximate buckling load, λ_M, for any given values of $\bar{p}$ and $\bar{\xi}_1$ corresponds to the value of γ such that λ given by (29) is a minimum.

With $\bar{p} = 0$, (29) is the equation Koiter used to plot an upperbound to the buckling load of an unpressurized shell with axisymmetric imperfections. This curve for $\nu = \frac{1}{3}$ is shown in Figure 3. For small values of $\bar{\xi}_1$ the minimum value of λ from (29) corresponds to values of γ in the neighborhood of unity and (29) becomes

$$2(1 - \lambda_M^\circ)^3 - (1 - \lambda_M^\circ)(2 + \lambda_M^\circ)c\bar{\xi}_1 + \frac{26}{25}(c\bar{\xi}_1)^2 = 0 \tag{30}$$

*An elaboration of this statement is found in Appendix I.

Equation (29) from the more approximate analysis is obtained if the $\bar{\xi}_1^2$ term in (30) is neglected; and thus as seen in Figure 3, the two curves approach each other for sufficiently small $\bar{\xi}_1$.

For non-zero values of $\bar{p}$ the minimum λ with respect to γ is found from (29) with the use of a digital computer. Three typical buckling load - pressure curves are shown in Figure 6. λ_M as obtained from (29) or this figure is an upperbound to the buckling load for a shell with the initial imperfection $\bar{\xi}_1$ and internal pressure corresponding to the parameter $\bar{p}$. The three curves of Figure 4 obtained on the basis of the approximate calculation do not differ appreciably from the upperbound curves of Figure 6, although the value of $\bar{\xi}_1$ associated with each approximate curve is smaller than the value associated with the corresponding upperbound curve. Use of the curves of Figure 5 would seem justified if one wishes to relate the buckling load of a pressurized cylinder to the buckling load of an unpressurized cylinder with similar initial imperfections.

The elastic buckling description is valid only as long as no plastic deformation occurs prior to buckling. The elastic hoop strain due to internal pressure alone is of the order $\bar{p}h/R$. Thus, in most cases plastic deformation will occur well before the pressure parameter attains the value 10. Clearly, the buckling load can remain below the classical value for the entire range of elastic buckling.

COMPARISON WITH SOME EXPERIMENTAL RESULTS

Recent tests with Mylar cylinders performed by Weingarten, Morgan and Seide (9) are particularly suited to comparison with the results obtained here. Mylar is able to suffer reasonably large strains prior to deforming plastically. Thus, Weingarten, et. al., were able to perform a series of tests at different internal pressures with the same specimen without incurring any plastic deformation.

Figure 7 presents two typical tests series and two theoretical curves chosen from Figure 5 which best fit the experimental data. Weingarten, et. al., did not report any information with respect to either the form or magnitude of the imperfection which would permit us to assign values to $\bar{\xi}_1$ and $\bar{\xi}_2$. Certainly the imperfection representation (12) assumed in the analysis could represent the true imperfection only in an average sense; and especially for $\bar{p} < 1$, a more exact description would require additional asymmetric terms. Nevertheless, the form of the experimental results can be reproduced by an appropriate a posteriori choice of $\bar{\xi}_1$ and $\bar{\xi}_2$.

The radius-thickness ratio of the previously mentioned tests ranged from 200 to 2000, with the maximum load of the unpressurized shells ranging from about .6 of the classical value at $R/h = 200$ to .3 at $R/h = 2000$. This R/h dependence is most readily interpreted in light of the present analysis by associating larger imperfections (relative to the shell thickness) with larger values of R/h. Indeed, it seems reasonable that such would be the case.

Judging from the results presented, the relative amount of the axisymmetric imperfection is small compared to the asymmetric imperfections in the Weingarten, et. al., test specimens. This is particularly the case for specimen 100.2, and the buckling load is only slightly below the classical value for $\bar{p} > 1$. Included in Figure 7 is data from a series of tests on axially loaded, pressurized aluminum cylinders performed at the D.V.L. and reported by Thieleman (2). In this series of tests, new specimens had to be used for each test; and although the radius and thickness were unchanged, there was undoubtedly some variation in initial imperfections from specimen to specimen as indicated by the data scatter. The important feature of these tests is that the buckling load remains well below the classical value for values of the pressure parameter well above unity. Axisymmetric initial imperfections are strongly suspected.

APPENDIX I

We have asserted that λ as obtained from equation (29) is an upper bound to the exact buckling load as predicted by equations (26) and (27). The following demonstration follows from Koiter's (6) general theory of elastic instability. The trivial (or prebuckling) deformation at a given value of load λ is denoted by w_s and is construed in a generalized sense. If w is any kinematically admissible deformation in addition to the prebuckling deformation w_s, then the change in potential energy of the structure is

$$P[w + w_s] - P[w_s] = P_2[w,\lambda] + P_3[w,\lambda] + \text{----}$$

where $P_n[w,\lambda]$ is a functional which is homogeneous and of nth degree in w. $P_1[w,\lambda]$ is zero since w_s is an equilibrium configuration. We have assumed w is sufficiently small to make this expansion meaningful.

At any value of the load parameter, λ, the structure is stable if

$$P_2(w,\lambda) > 0 \qquad \text{for all admissible } w$$

Thus, if for any λ_a and admissible w_a,

$$P_2(w_a,\lambda_a) = 0 \tag{A-1}$$

then obviously $\lambda_a \geq \lambda_c$ where λ_c is the lowest value of λ such that there exists an admissible w for which $P_2(w,\lambda) = 0$.

In the present case the terms in the brackets of equations (24) and (25) constitute the exact trivial solution w_s. Equations (26) and (27) are equivalent to the Euler equations for minimizing $P_2(w,\lambda)$. Since we have solved the compatibility equation exactly in terms of the assumed radial component of the

shell displacement, the stresses are derived from an admissible displacement field. The Galerkin solution to the equilibrium equation is equivalent to an approximate Raleigh-Ritz minimalization of $P_2(w,\lambda)$. That is, if the additional admissible displacement which we have assumed is denoted by ξw_a , then the approximate eigen-value λ_a is found by

$$\frac{\partial}{\partial \xi} P_2(\xi^2 w_a, \lambda_a) = 2\xi P_2(w_a, \lambda_a) = 0$$

Thus by (A-1) $\lambda_a \geq \lambda_c$.

REFERENCES

1. Lo, H., Crate, H. and Schwartz, E. B., "Buckling of Thin-Walled Cylinder Under Axial Compression and Internal Pressure", NACA TR 1027, 1951.
2. Thielemann, W. F., "New Developments in the Non-linear Theories of the Buckling of Thin Cylindrical Shells", Aeronautics and Astronautics, Pergamon Press, pp. 76-121, New York (1960).
3. Lu, S. V. and Nash, W. A., "Buckling of Initially Imperfect Axially Compressed Cylindrical Shells", NACA, TN D-1510 (1962).
4. Hoff, N. J., "The Effect of Edge Conditions on the Buckling of Thin Walled Circular Shells in Axial Compression", to be published in the Proceedings of the Eleventh International Congress of Applied Mechanics, August 1964.
5. Koiter, W. T., "On the Stability of Elastic Equilibrium" (in Dutch with English summary) Thesis Delft, H. J. Paris, Amsterdam (1945).
6. Koiter, W. T., "Elastic Stability and Post-buckling Behavior", Proceedings Symposium Non-linear Problems, edited by R. E. Langer, University of Wisconsin Press, 257-275 (1963).
7. Budiansky, B. and Hutchinson, J., "Dynamic Buckling of Imperfection-Sensitive Structures", to be published in Proceedings of the Eleventh International Congress of Applied Mechanics (1964).
8. Koiter, W. T., "The Effect of Axisymmetric Imperfections on the Buckling of Cylindrical Shells under Axial Compression", Koninkl. Nederl. Akademie Van Weterschappen - Amsterdam, Series B, 66, No. 5 (1963).
9. Weingarten, V. I., Morgan, E. J., and Seide, P., "Final Report on Development of Design Criteria for Elastic Stability of Thin Shell Structures", S.T.L. Report, December 1960.

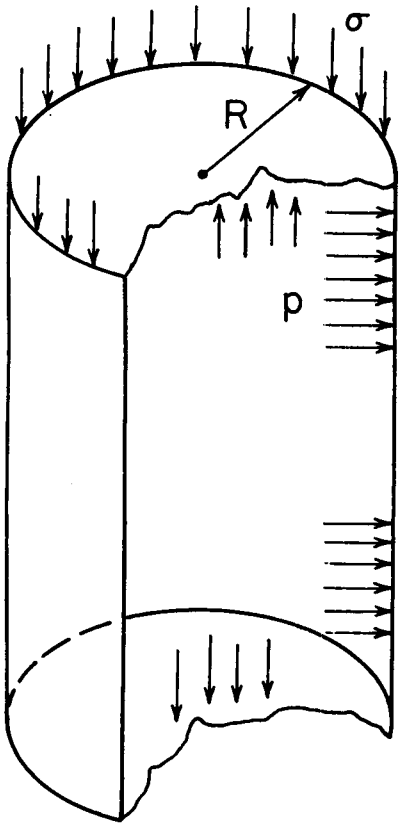

YOUNG'S MODULUS, E
POISSON'S RATIO, ν
SHELL THICKNESS, h

FIGURE 1

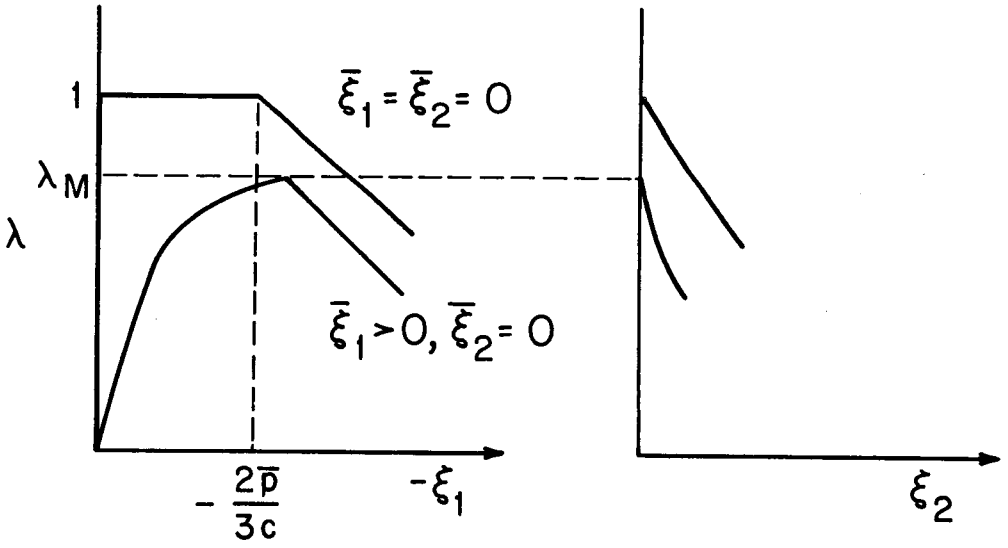

FIGURE 2

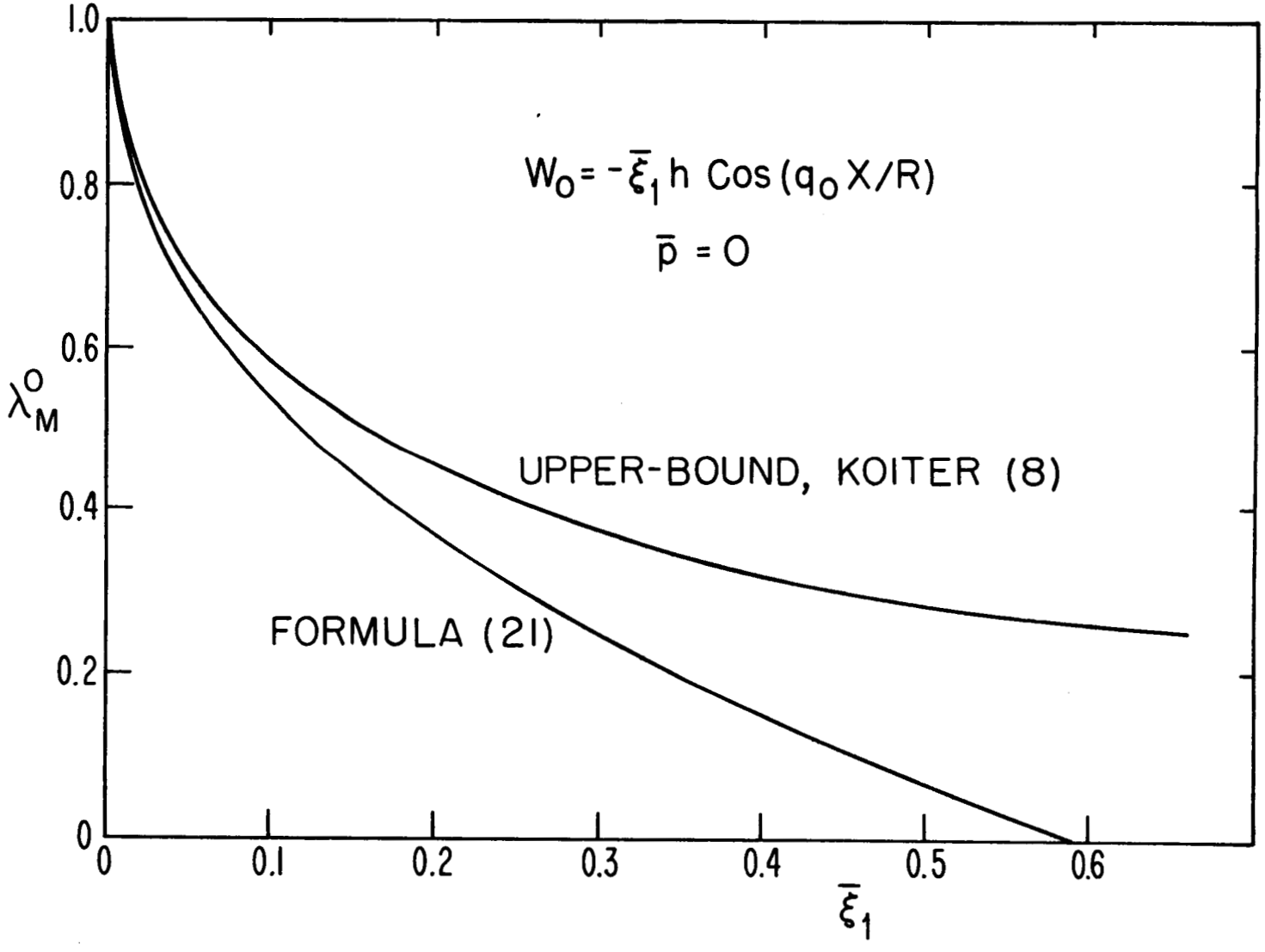

FIG. 3. EFFECT OF AXISYMMETRIC IMPERFECTION ON BUCKLING OF UNPRESSURIZED SHELL.

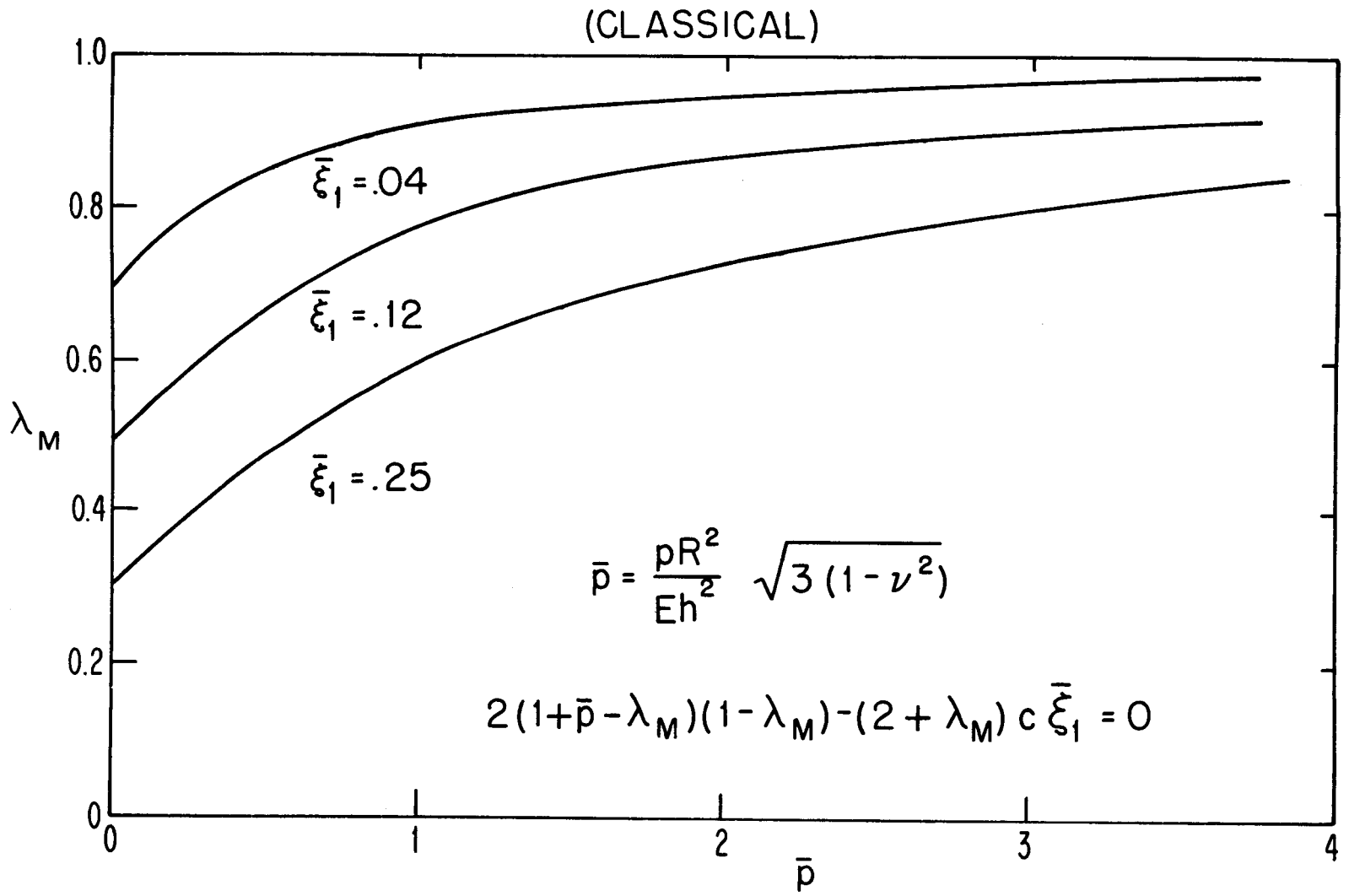

FIG. 4. EFFECT OF AXISYMMETRIC IMPERFECTION ON BUCKLING OF PRESSURIZED SHELL.

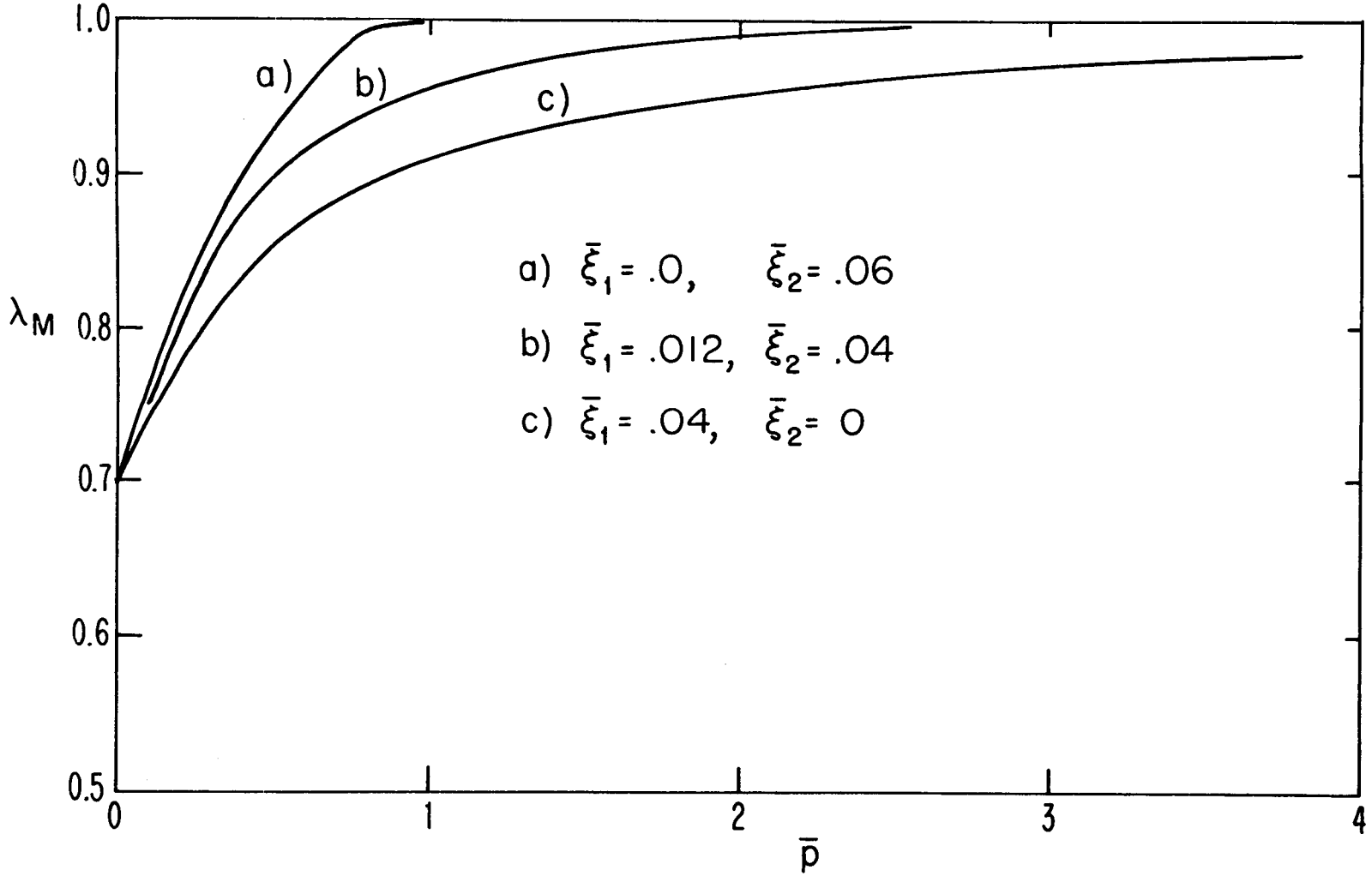

FIG. 5a EFFECTS OF AXISYMMETRIC ($\bar{\xi}_1$) AND ASYMMETRIC ($\bar{\xi}_2$) IMPERFECTIONS.

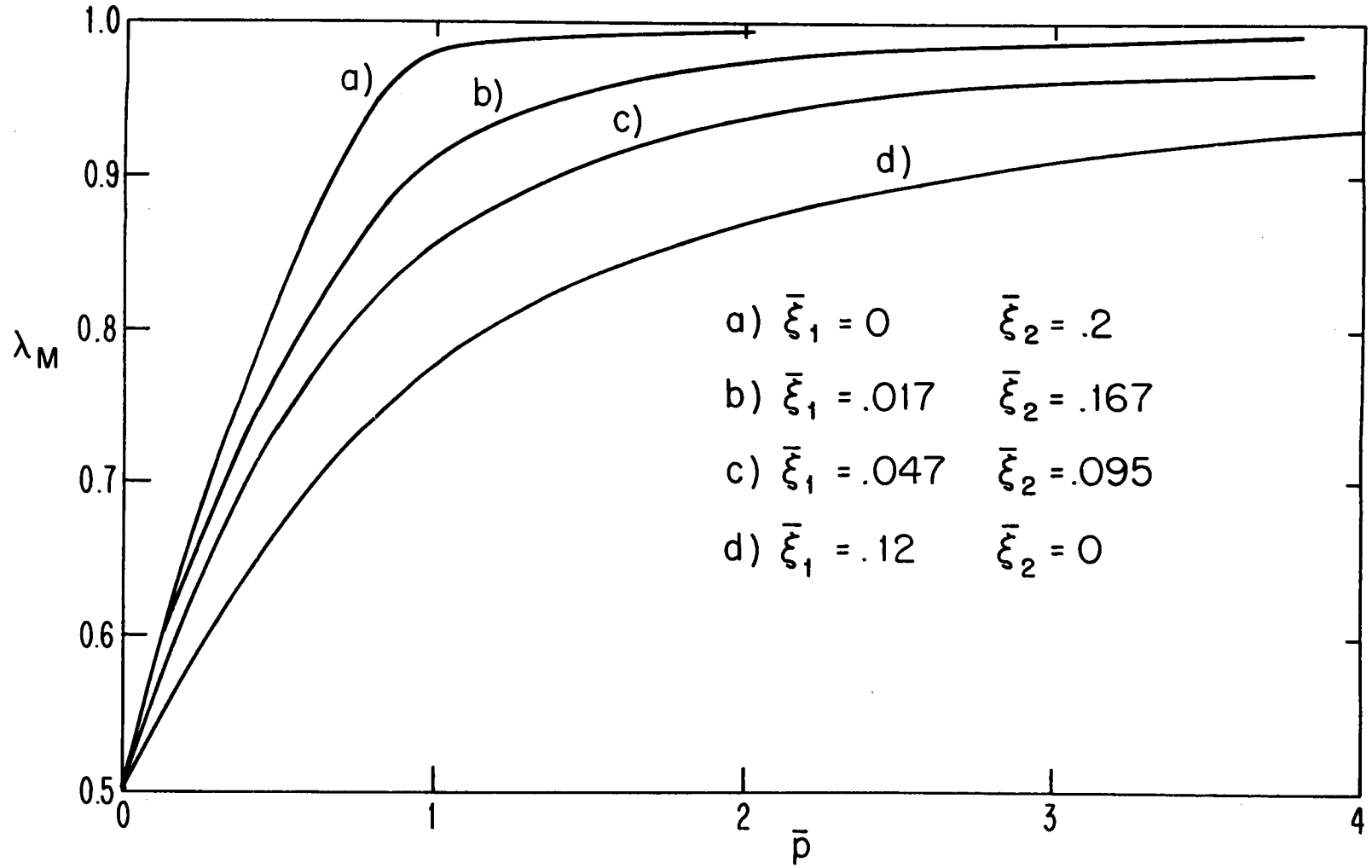

FIG. 5b EFFECTS OF AXISYMMETRIC ($\bar{\xi}_1$) AND ASYMMETRIC ($\bar{\xi}_2$) IMPERFECTIONS.

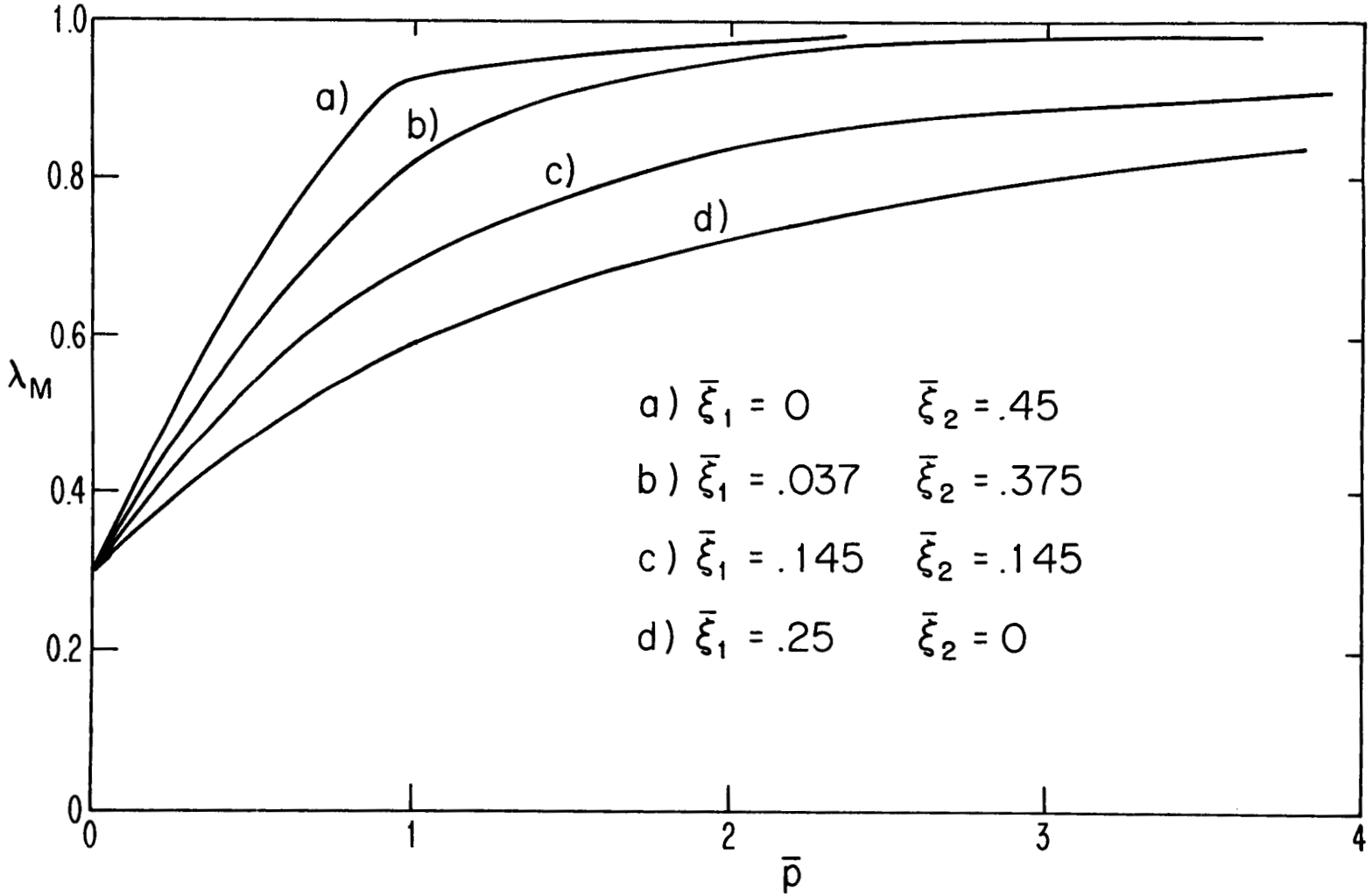

FIG. 5c EFFECTS OF AXISYMMETRIC ($\bar{\xi}_1$) AND ASYMMETRIC ($\bar{\xi}_2$) IMPERFECTIONS.

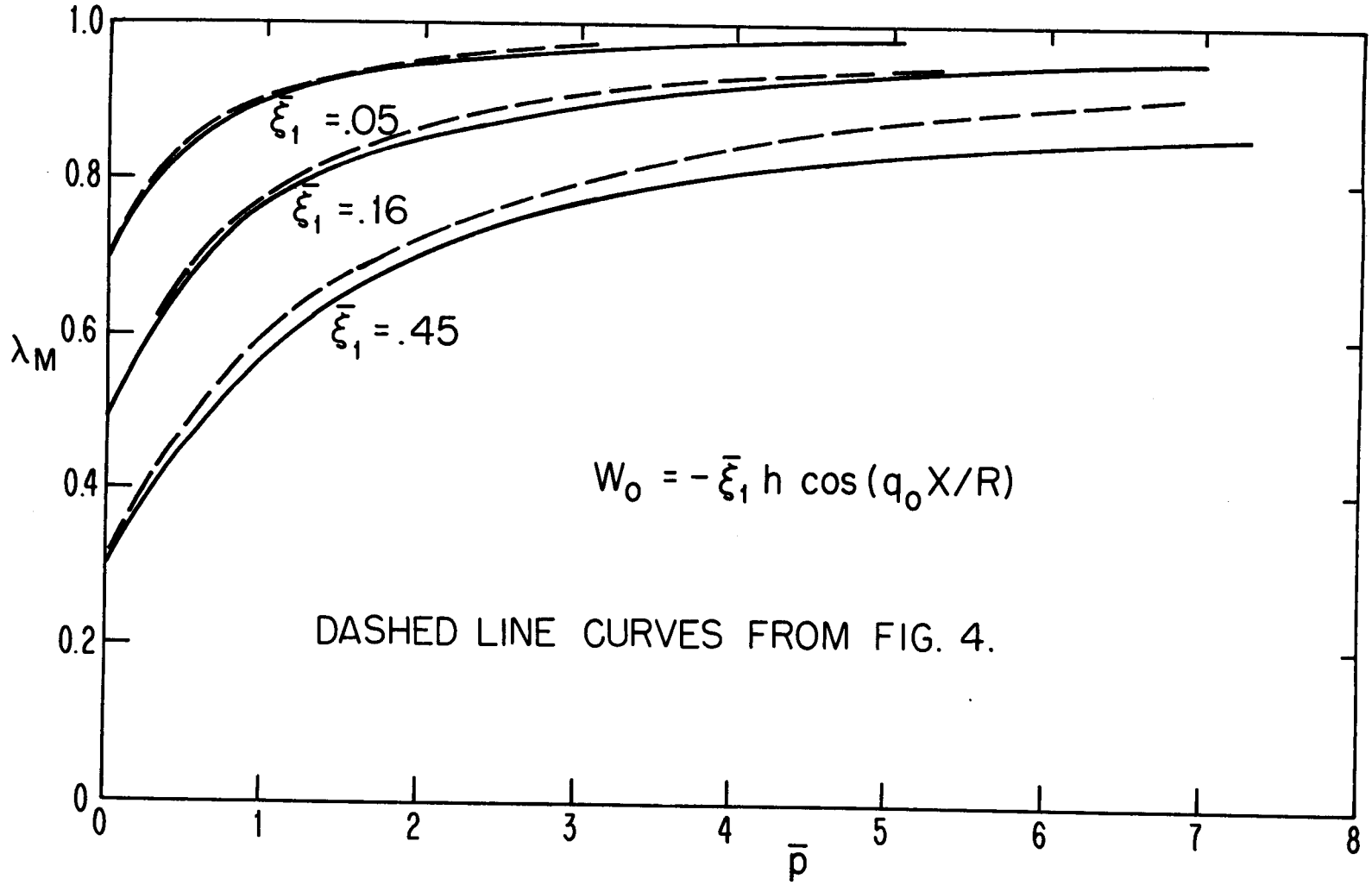

FIG. 6 UPPER-BOUND TO BUCKLING LOAD FOR PRESSURIZED CYLINDER WITH AXISYMMETRIC IMPERFECTION.

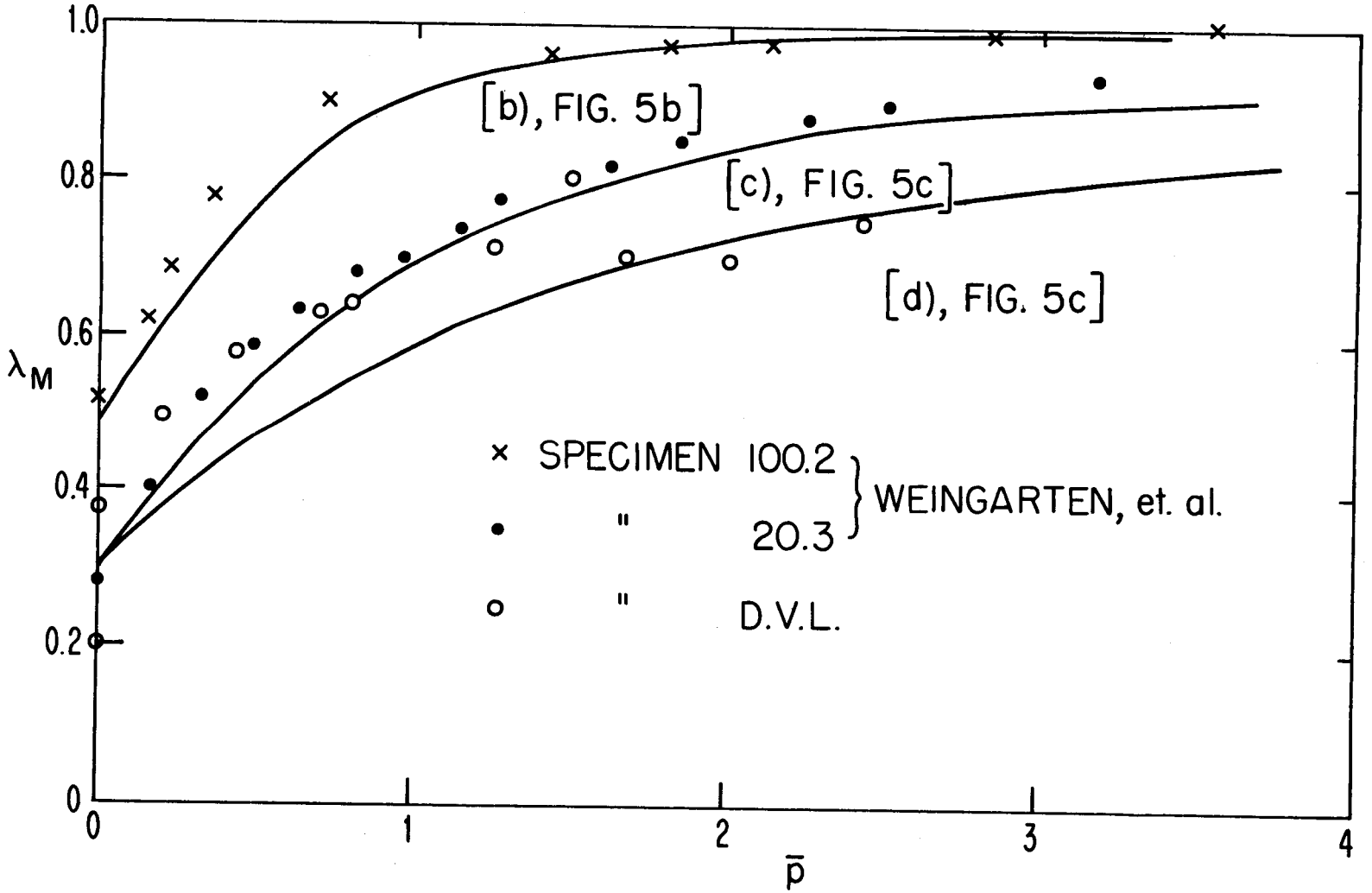
1.0
0.8
0.6
0.4
0.2
0
λ_M
0
1
2
3
4
$\bar{p}$
[b), FIG. 5b]
[c), FIG. 5c]
[d), FIG. 5c]
× SPECIMEN 100.2
• " 20.3
o " D.V.L.
} WEINGARTEN, et. al.

FIGURE 7